Plant Soil (2018) 422:169–181
DOI 10.1007/s11104-017-3294-x

REGULAR ARTICLE

Proteomic analysis of responsive root proteins of *Fusarium oxysporum*-infected watermelon seedlings

Man Zhang · Jinhua Xu · Guang Liu · Xiefeng Yao · Runsheng Ren · Xingping Yang

Received: 27 December 2016 / Accepted: 22 May 2017 / Published online: 24 July 2017

Abstract
Aims Fusarium oxysporum is a causal disease that threatens watermelon production, but little information on the molecular mechanisms involved in host defense is available. To understand the defense response, a proteome-level changes that occur in watermelon roots during *F. oxysporum* infection were investigated.
Methods We utilized two-dimensional gel electrophoresis (2-DE) to compare changes in the root proteome profiles and validated their expression using real-time PCR.
Results A total of 690 spots were detected, and 32 proteins had significant changes in abundance and were further identified by mass spectrometry. These proteins were mainly involved in metabolism, stress and defense and amino acid biosynthesis. RT-PCR analysis revealed that transcripts corresponding to the nine randomly selected proteins could be significantly induced, their expression patterns were consistent with the proteomic results except for *Apx* and *Tdh*. The involvement of these proteins in regulating watermelon response against *F. oxysporum* is discussed.
Conclusions The reprogrammed proteins were involved in several biological processes, which indicates that watermelon can directly alter the abundance of these proteins to establish a defense response. This work helps us understand the basic processes during the watermelon-*F. oxysporum* interaction and may contribute to improve resistance breeding toward this pathogen.

Keywords *Citrullus lanatus* · *Fusarium oxysporum* f.sp. *niveum* · Proteome · Root · 2-de · Gene expression

Responsible Editor: Stéphane Compant.

Electronic supplementary material The online version of this article (doi:10.1007/s11104-017-3294-x) contains supplementary material, which is available to authorized users.

M. Zhang · J. Xu (✉) · G. Liu · X. Yao · R. Ren · X. Yang
Jiangsu Key Laboratory for Horticultural Crop Genetic Improvement/Institute of Vegetable, Jiangsu Academy of Agricultural Sciences, Nanjing, Jiangsu, China
e-mail: jinhuaxu@jaas.ac.cn

Introduction

Fusarium oxysporum f.sp. *niveum*, causing fusarium wilt, is the causal agent of watermelon (*Citrullus lanatus* (Thunb.) Matsum. & Nakai) in many areas of the world (Martyn 1996). According to the differences in virulence, isolates of *F. oxysporum* f.sp. *niveum* are subdivided into four physiological races, namely, race 0, 1, 2 and 3 (Zhou et al. 2010). *F. oxysporum* can survive in soil for 11 or more years by producing chlamydospores (Garrett 1970), and is thus difficult to control. *F. oxysporum* infects watermelon plants at all stages and leads to the damp-off of seedlings and wilt of plants, resulting in death (Martyn 1996). Infection by *F. oxysporum* causes severe economic losses in watermelon crops and limits watermelon production. Therefore, it is believed to be the most destructive disease in watermelon.

Plants can initiate a series of resistance mechanisms to prevent the invasion of fungi and suppress their growth within host tissues (Moreira et al. 2013) to

maintain cellular homeostasis and defend against fungi attack. To date, numerous studies have explored defense mechanisms during the watermelon and *F. oxysporum* interaction. Strategies for pathogen resistance include addressing: (1) the histological features of infection by *F. oxysporum*, via the formation of gums and tyloses in vascular tissue and vascular cavities (Baayen et al. 1989; Zhang et al. 2015a); (2) the effects of different rootstocks on *F. oxysporum* incidence (King et al. 2008); (3) the physiological and biochemical responses of watermelon to *F. oxysporum* infection via enhanced levels of defense enzymes and PR proteases (Zhang et al. 2015b); and (4) the induced expression of defense-related genes (Zhang et al. 2015a). Based on the whole genome sequencing of watermelon, three major classes of disease-resistance genes, including 44 nucleotide-binding sites and leucine-rich repeats (NBS-LRR) and 26 lipoxygenase (LOX) and 197 receptor-like genes, in the watermelon genome were identified (Guo et al. 2013). More recently, a major quantitative trait locus (QTL) associated with Fon race 1 resistance was identified in watermelon, and eight candidate resistance genes were found within the confidence interval of the identified QTL (Meru and McGregor 2016). However, the molecular mechanisms of the responses of watermelon plants infected by *F. oxysporum* are still not well understood. Therefore, a thorough analysis of watermelon defense mechanisms is required.

Proteomic analysis has advanced the monitoring of global changes in protein abundance under stress and has thus been widely applied to investigate plant defense responses to various stress factors (Afroz et al. 2011). In watermelon, proteomic-based analysis has been used to investigate proteomic response mechanisms under abiotic stresses such as drought (Yoshimura et al. 2008) and salinity (Yang et al. 2012). Data from these studies contributed to understanding the complex molecular defense mechanisms of watermelon to abiotic stresses. However, the molecular mechanisms of watermelon defense against biotic stress, particularly *F. oxysporum*, are still limited.

In this work, we conducted a proteomic analysis in watermelon after *F. oxysporum* infection to investigate the watermelon-*F. oxysporum* interaction. Root proteins were extracted and analyzed using two-dimensional gel electrophoresis (2-DE). Thirty-two proteins showed statistically significant differences in abundance and were classified into 6 different functional categories. The expression profiles of transcripts corresponding to 9 identified proteins at 4 time points (12, 24, 48, 240 h after inoculation) were analyzed using real-time PCR. This work identified proteins that significantly respond to *F. oxysporum* in watermelon roots and thus provides insight into the molecular mechanisms that are involved in the response to *F. oxysporum* infection in watermelon.

Materials and methods

Plant materials and fungal growth

Watermelon cv. Sumi No. 1 (SM1), which is sensitive to *Fusarium oxysporum*, was provided by the Institute of Vegetable Crops, Jiangsu Academy of Agricultural Sciences, China. Seeds of SM1 were germinated in an incubator at 28 °C and then incubated in a growth chamber at 30/15 °C (day/night). Twenty-day-old seedlings were used for fungal inoculation. Non-inoculated roots (as control) and roots inoculated at 10 days post inoculation (dpi) were sampled for proteomic analysis; samples were immediately frozen in liquid nitrogen and stored at −80 °C. A total of 10 roots were pooled for each sample. The experiment was repeated to obtain three biological replicates.

The *F. oxysporum* race 1 isolate, provided by the Institute of Vegetable Crops, Jiangsu Academy of Agricultural Sciences, China, was maintained on potato dextrose agar (PDA) at 25 °C. Seven-day-old cultured fungus was used for inoculation.

Preparation of inoculum and inoculation of plants

Fungal suspensions were grown in a 250-mL triangular flask with 150 mL liquid PDA medium at 25 °C on a rotary shaker at 150 rpm for 5–7 days. The concentration of conidia in the suspension culture was adjusted to 10^6 conidia per mL for plant inoculation with sterile distilled water. Twenty-day-old seedlings were carefully removed from the aperture disk and gently swirled in tap water to wash away soil particles. Roots were immersed in a freshly prepared spore suspension (10^6 conidia mL^{-1}) for 30 min. The inoculated seedlings were replanted in peatmoss + vermiculite + perlite (6:1:3, *v*/v/v) growth medium. Control plants were treated as above but were immersed in sterile distilled water (Chang et al. 2008).

Microscopic examination

To observe the vascular structure, SM 1 roots were sampled at 10 dpi and washed carefully to remove the soil. A total of 6 plants were taken for each sample. The sampled roots were sectioned to lengths of 5 mm, fixed in 2.5% glutaraldehyde and 0.2 M phosphate buffer (pH 7.2) and placed under vacuum to remove any remaining air. Subsequently, the samples were dehydrated with gradient ethanol and critical-point dried according to the methods described by Fernández-García et al. (2004). The samples were coated with gold in a Model E-1010/E-1020 Hitachi Ion Sputter Jeol (Japan) and observed using an XL30 ESEM (Philips, Holland).

Protein extraction and two-dimensional gel electrophoresis (2-DE)

Total proteins were extracted from root samples of SM1. Root samples were ground in liquid nitrogen, and the tissue powder produced was immediately suspended in an extraction buffer containing 9.5 M urea, 4% *w*/*v* 3-[(3-cholamidopropyl) dimethylammonio]-1-propanesulfonate (CHAPS), 65 mM dithiothreitol (DTT), and 2% *v*/v immobilized pH gradient (IPG) buffer pH 3–10. Crude homogenates were centrifuged at 4 °C (13,000×g for 30 min). The supernatants were precipitated overnight at −20 °C in 30 mL of cold acetone supplemented with 10% (*v*/v) TCA and 0.07% β-mercaptoethanol, followed by centrifugation at 13,000×g for 30 min. The pellets were resuspended with 10 mL of cold acetone containing 0.07% β-mercaptoethanol, mixed vertically, precipitated at −20 °C for 30–60 min and centrifuged at 13,000×g for 30 min at 4 °C. This step was repeated twice. The protein pellets were allowed to air dry at room temperature and stored at −80 °C. Protein contents were determined by the Bradford method (Bradford 1976) using bovine serum albumin as the standard.

Protein (800 μg for each sample) was loaded onto a 13 cm rehydration strip with an immobilized pH gradient of 4–7 and separated on a Multiphor electrophoresis unit (GE Healthcare, Tokyo, Japan) using the following program: 30 V for 12 h; 1 h step from 200 V–500 V; 1 h gradient from 500 to 1000 V; 30 min gradient from 1000 to 4000 V; 30 min gradient from 4000 to 8000 V; and 5 h at 8000 V. After isoelectric focusing (IEF), the rehydration strip was balanced twice in reducing buffer containing 6 M urea, 50 mM Tris-HCl (1.5 M stocking buffer, pH 8.8), 30% glycerol, 2% sodium-dodecyl sulphate (SDS), 1% dithiothreitol (DTT) or 4% iodoacetamide (IAA). The strip was transferred to the top of a 10% SDS-polyacrylamide gel covered with 0.5% low melting point agarose gel in a Hoefer SE 600 Ruby system (GE Healthcare, Tokyo, Japan). Electrophoresis was performed at a constant current of 5 mA per gel for 15 min and 10 mA per gel for 6 h. Gels were stained with Coomassie blue G-250, and scanned using a TyphoonTM 9400 imager (GE Healthcare, Tokyo, Japan). The scanned images were applied to ImageMaster 2D Platinum 6.0 software (GE Healthcare, Tokyo, Japan). Protein spots exhibiting differential abundance were identified by Student's *t*-test of spot intensity ($P < 0.05$) and were then digested with modified trypsin (Promega, USA) and analyzed by MALDI-TOF/TOF. Proteins were identified by searching the NCBInr database with a Viridiplantae (green plants) restriction and EST_cucurbitaceae using the Mascot search tool (Matrix Science, London, UK). The protein-protein interaction (PPI) network was analyzed via the STRING v.10 online program (http://string-db.org/). Subcellular localizations of the proteins identified as significant differences in abundance were predicted using WoLF PSORT (http://www.genscript.com/wolf-psort.html).

Quantitative real-time RT-PCR

Total RNA was extracted from roots of SM 1 inoculated by *F. oxysporum* at 0, 12, 24, 48 and 240 h after inoculation (hai) using a RNApure Plant kit (with DNaseI) (CWBiotech, China). A BU-Superscript RT kit (Biouniquer, China) was used for generation of first-strand cDNA. Real-time PCR was carried out using 1 x SYBR Green PCR Master Mix (PE Applied Biosystems, USA) in the GeneAmp® 7300 Sequence Detection System (PE Applied Biosystems, USA) according to the manufacturer's instructions. *18SrRNA* (GenBank accession number AB490410) was used as the internal control for normalization. The relative expression levels were calculated using the $2^{-\Delta\Delta CT}$ method (Livak and Schmittgen 2001). Primer sequences used in this study were shown in Supplementary Table S2.

Results

Wilting symptoms in watermelon seedlings

Visual wilting symptoms were observed in watermelon seedlings at 10 d after inoculation (DAI) (Fig. 1a). In *F.*

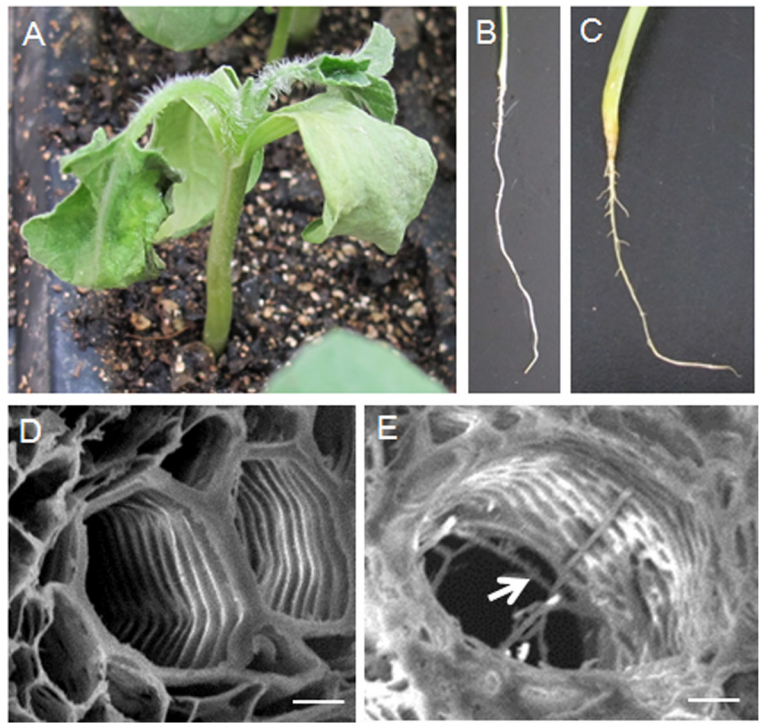

Fig. 1 Inoculation of watermelon seedlings with *F. oxysporm*. **a** Conidial suspension-treated watermelon seedling at 10 dpi. Healthy roots (**b**) and roots inoculated with *F. oxysporm* (**c**). Cross section of healthy roots (**d**) and roots inoculated with *F. oxysporm* (**e**). Arrow shows hyphae. Scale bars indicate 200 μm (**d, e**)

oxysporum-inoculated plants, roots were noted as brown (Fig. 1c) compared to healthy roots (Fig. 1b). Moreover, roots of healthy and *F. oxysporum*-infected watermelon seedlings were examined internally using an electron microscope. Cross-sectional photomicrographs of root tissues showed that the hyphae of *F. oxysporum* infiltrated into the xylem vessel (Fig. 1e), whereas healthy roots were hyphae-free (Fig. 1d).

Identification of *F. oxysporum*-responsive root proteins using two-dimensional electrophoresis

The defense response of watermelon roots against *F. oxysporum* was investigated. Changes in the root proteins at 10 DAI were analyzed using two-dimensional electrophoresis (2-DE). Total protein was extracted from healthy and *F. oxysporum*-inoculated watermelon roots, respectively, and subjected to 2-DE. Representative 2-DE gels are shown in Fig. 2. Approximately 1300 protein spots were obtained after a combined analysis of IEF using a pH 4–7 NL IPG strip and SDS-PAGE, and 690 protein spots were matched between mock- and *F. oxysporum*-inoculated groups. Statistical analysis (1.5-fold change at a p-value <0.05) revealed 32 protein spots had significant changes in abundance (Fig. 2). Compared to those proteins that were identified from mock-treated watermelon seedlings, 18 proteins from *F. oxysporum*-inoculated watermelon seedlings were more abundant and 14 were less abundant.

Characterization of differentially represented proteins in SM1 infected with *F. oxysporum*

Spots of the 32 proteins showed significant differences in abundance were excised from the corresponding gels and digested with trypsin. In total, 32 spots were successfully identified by MALDI-TOF/TOF (Table 1). The functional categories of the identified proteins were further investigated and showed that these proteins are involved in metabolism (10), stress and defense (11), amino acid biosynthesis (7), signal transduction (2) and transport and cell structure (2).

Among the 10 proteins involved in metabolism, three enzymes encoding vacuolar H^+-ATPase catalytic subunit A (spot s1), pyruvate dehydrogenase E1 component subunit beta (spot s29) and phosphoglycerate kinase (spot s32) were involved in energy metabolism pathway. Three enzymes, succinate dehydrogenase flavoprotein subunit (spot s2), NADP-dependent malic enzyme (spot s21) and isocitrate dehydrogenase (spot s22), participate in carbohydrate metabolism. Proteins related to stress

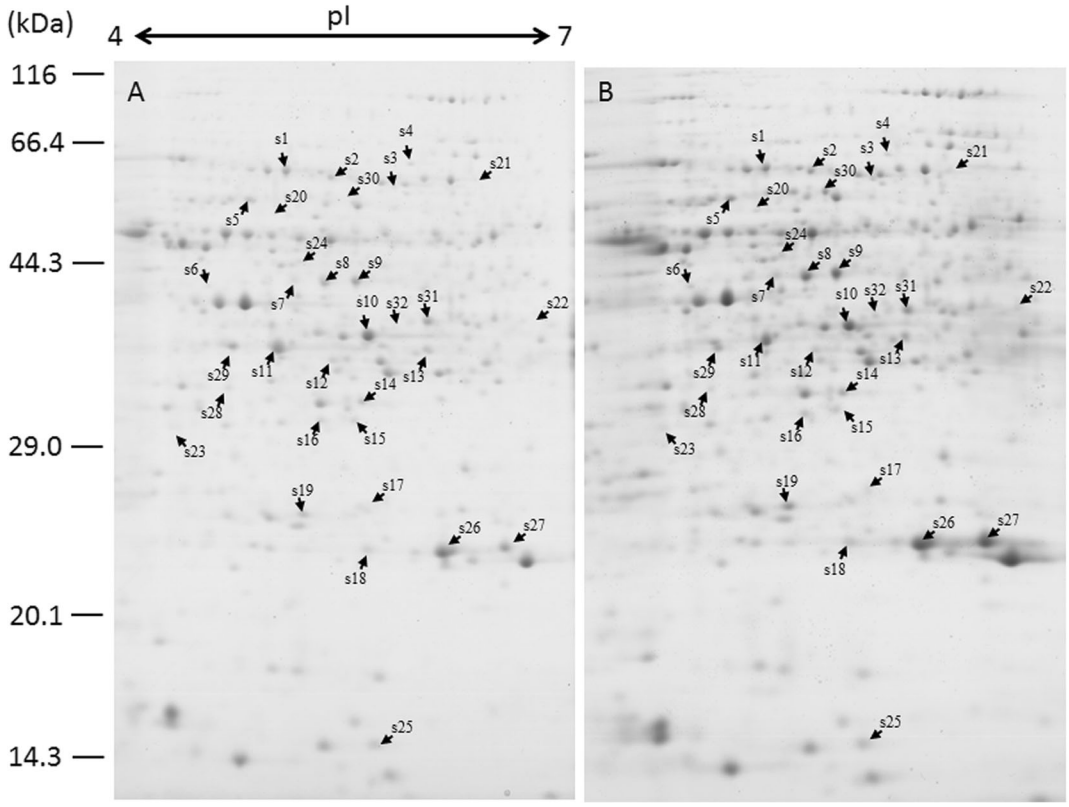

Fig. 2 Representative 2-D gels of proteins extracted form watermelon roots with mock-inoculated (**a**) and infected with *F. oxysporum* (**b**) at 240 hai. 800 μg proteins were focused on IPG strips (11 cm), pH 4–7NL, and separated by SDS-PAGE (12.5%). The experiment was repeated 3 times

and defense were the largest group, including heat shock protein (spot s4), 2 peroxidases (spots s11, s31), 2 jasmonate-induced proteins (spots s18, s27), NAD(P)H dehydrogenase (quinone) FQR1-like 2 (spot s15), and chaperonin CPN60–2 (spot s5). Seven proteins are involved in amino acid biosynthesis and correspond to 3 S-adenosylmethionine synthases (spots s7, s8, s9). In relation to signal transduction, representation of gibberellin receptor GID1L2 (spot s14) and tyrosine-protein kinase (spot s24) were decreased after *F. oxysporum* infection.

Moreover, subcellular localization showed that the 32 identified proteins are localized to the cytoplasm (12), cytoskeleton (4), chloroplast (7), mitochondrion (5), nucleus (2), extracellular (1) and endoplasmic reticulum (1) (Fig. 3). The subcellular localization gives information about protein physiological function, and the prediction results indicate that cytoplasmic proteins (50%) are mainly involved in plant defense against *F. oxysporum* in watermelon.

Protein-protein interactions network

Proteins perform their functions by relying on an interaction network in association with other proteins that are integral to cellular processes (Miernyk and Thelen 2008). To determine interaction information for *F. oxysporum*-responsive proteins, the 32 proteins had significant changes in abundance were analyzed online using the STRING database. Their functional partners and interactions were demonstrated (Fig. 4). As expected, most differentially represented proteins were mutually interactive. Proteins for amino acid biosynthesis, stress and defense, carbohydrate metabolism and energy metabolism constituted a complex interactive network (Fig. 4, Supplementary Table S1). Among the proteins, HSP60 (chaperonin CPN60), SDH1–1 (succinate dehydrogenase) and PGK (phosphoglycerate kinase) were strongly interactive with other proteins. This observation led us to speculate that these proteins might function cooperatively with each other in watermelon

Table 1 Identification of differentially represented proteins in SM1 roots inoculated with *F. oxysporum*

Spot	Protein description	Watermelon accession	Mr (KD)/pI	Coverage%	Score	Cell compartment	Protein fold change (*F. oxysporum* infected/control)[a]
Energy and metabolism related							
S12	Quinone oxidoreductase-like protein	Cla010398	34.385/5.76	28	311	Cytoplasm	0.66
S16	Epoxide hydrolase	Cla017397	35.109/5.52	10	110	Chloroplast	0.63
S17	Acid phosphatase	Cla005951	29.877/5.91	20	221	Mitochondrion	1.02
S28	Nitrile-specifier protein	Cla010432	35.274/5.15	25	461	Cytoplasm	0.44
S1	Vacuolar H^+-ATPase catalytic subunit A	Cla015485	68.683/5.36	20	564	Chloroplast	0.68
S29	Pyruvate dehydrogenase E1 component subunit beta	Cla001493	45.725/8.019	11	339	Chloroplast	1.02
S32	Phosphoglycerate kinase	Cla005491	40.610/5.43	27	456	Cytoplasm	0.54
S2	Succinate dehydrogenase flavoprotein subunit	Cla001940	64.964/5.42	12	177	Cytoplasm	0.68
S21	NADP-dependent malic enzyme	Cla011268	61.960/6.62	8	128	Endoplasmic reticulum	1.78
S22	Isocitrate dehydrogenase	Cla010418	40.039/8.98	2	54	Chloroplast	2.35
Amino acid biosynthesis							
S3	Aspartate-tRNA synthetase	Cla020930	60.971/5.73	21	453	Nucleus	0.74
S7	S-adenosylmethionine synthase	Cla017324	43.034/5.50	23	294	Cytoplasm: cytoskeleton	0.74
S8	S-adenosylmethionine synthase	Cla017324	43.034/5.50	23	294	Cytoplasm: cytoskeleton	0.89
S9	S-adenosylmethionine synthase 1	Cla015190	43.149/5.58	20	384	Cytoplasm: cytoskeleton	0.88
S10	Glutamine synthetase	Cla015195	39.244/6.72	14	485	Cytoplasm	0.67
S25	40S ribosomal protein S12	Cla015328	14.851/5.76	37	131	Cytoplasm	4.83
S30	Threonine dehydratase biosynthetic	Cla018349	66.977/6.79	13	463	Mitochondrion	1.78
Stress and defense							
S4	Heat shock protein STI	Cla005680	65.087/5.78	10	323	Cytoplasm	0.32
S5	Chaperonin CPN60–2, mitochondrial	Cla007630	61.064/5.84	5	134	Mitochondrion	0.90
S6	SGT1 protein	Cla006134	40.978/5.25	6	70	Cytoplasm	0.89
S11	Peroxidase	Cla003193	35.313/5.71	25	463	Extracellular	0.57
S19	Ascorbate peroxidase	Cla013254	27.274/5.60	24	390	Chloroplast	1.31
S31	Peroxidase	Cla003191	42.211/8.60	19	244	Chloroplast	4.83
S13	Aldo-keto reductase 1	Cla016930	38.003/5.86	19	335	Cytoplasm: cytoskeleton	1.17
S26	Flavoprotein WrbA	Cla001332	22.479/5.41	24	171	Mitochondrion	1.20
S15	probable NAD(P)H dehydrogenase (quinone) FQR1-like 2	Cla014192	28.095/5.88	11	180	Nucleus	0.94
S18	Jasmonate-induced protein	Cla016932	23.67/5.95	15	133	Cytoplasm	1.54
S27	Jasmonate-induced protein	Cla002537	21.955/6.18	28	335	Cytoplasm	1.49
Signal transduction							

Table 1 (continued)

Spot	Protein description	Watermelon accession	Mr (KD)/pI	Coverage%	Score	Cell compartment	Protein fold change (*F. oxysporum* infected/control)[a]
S14	Gibberellin receptor GID1L2	Cla010253	35.271/5.65	27	356	Cytoplasm	0.72
S24	Leucine-rich repeat receptor-like protein kinase	Cla022593	48.893/10.01	5	86	Chloroplast	0.70
Transport and cell structure							
S20	Tubulin alpha-3 chain	Cla017164	49.625/4.95	26	619	Cytoplasm	1.06
S23	Alpha-soluble NSF attachment protein 2	Cla006615	30.262/4.97	19	223	Mitochondrion	1.62

[a] The ratio of *F. oxysporum*/control shows the fold-change in spot abundance between *F. oxysporum* -inoculated roots and mock-treated roots for each protein. Data are representative of three independent experiments

resistance. However, this hypothesis need to be further experimental confirmation. Thus, we hypothesize that the interactions of proteins in this network might play critical roles in watermelon resistance to *F. oxysporum*.

Analysis of the expression profiles of the mRNAs of some identified proteins by real-time PCR.

To validate whether the gene expression profile at the transcription level was consistent with changes in protein level, nine proteins identified as being significantly represented were randomly selected for further real-time PCR analysis. RNA of the root samples at 12, 24, 48, 240 hai was extracted, followed by real-time PCR analysis. The expression patterns of the nine genes were summarized in Fig. 5. The transcript levels of *Sam*, *Pod*, *Gid1l2* and *Apx* decreased considerably upon *F. oxysporum* infection. The expression level of *Jip23* increased significantly upon *F. oxysporum* infection. The transcriptional expressions of *Hsp* and *Pgk* increased at 48 hai and decreased at 240 hai. Although *Ycp4* and *Tdh* exhibited opposite expression patterns, their expression decreased in 48 hai and increased at 240 hai. Comparing the expression patterns at 240 hai observed using real-time PCR and 2-DE, we found that the gene expressions in transcript level was not necessarily consistent with that at the protein level. Two of the nine genes, *Apx* and *Tdh*, showed opposite expression patterns in the two analyses. The abundance of APX increased in protein level (1.31-fold higher) but the expression of *Apx* was down-regulated in transcript level (2.86-fold lower). The protein abundance of TDH increased 1.78-fold at 10 dpi, but its expression level in mRNA decreased approximately 1.23-fold.

Discussion

Proteins related to energy and metabolism

Plants employ a number of defense mechanisms to defend against biotic and abiotic challenges, among which metabolic alteration is a common response during plant-pathogen interaction (López-Gresa et al. 2009). In this work, most proteins were involved in metabolism, which indicated their importance in watermelon defense against *F. oxysporum*. Plants try hard to maintain energy and metabolic homeostasis, which suggests an intimate connection between energy availability and stress tolerance (Baena-González and Sheen 2008). Previous work suggested that changes in carbohydrate metabolism were correlated with energy allocation in plant defense (López-

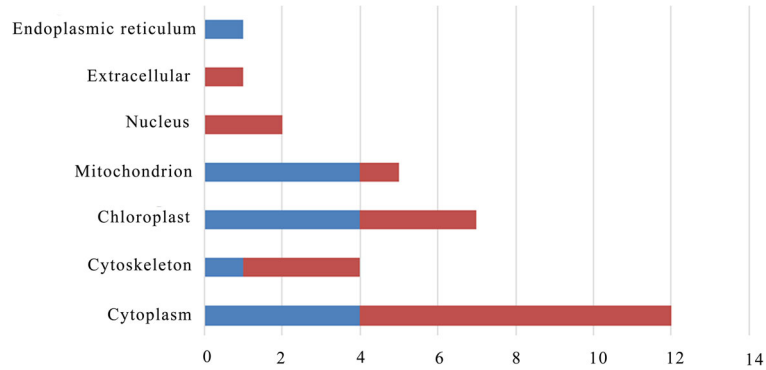

Fig. 3 Subcellular localizations of the 32 proteins with significant differences in abundance. Blue bars indicate over-represented proteins. Red bars indicate under-represented proteins. The x-axis shows the number of differentially represented proteins. The y-axis shows subcellular locations

Gresa et al. 2009). This hypothesis is supported in our work by the activation of three carbohydrate metabolism-related enzymes (spots s2, s21, s22) in *F. oxysporum*-infected watermelon. The over-representation of dehydrogenase E1 component subunit beta (spot s29), which is a major regulator of glucose oxidation (Stenlid et al. 2014), demonstrated increased energy demand during watermelon-*F. oxysporum* interaction.

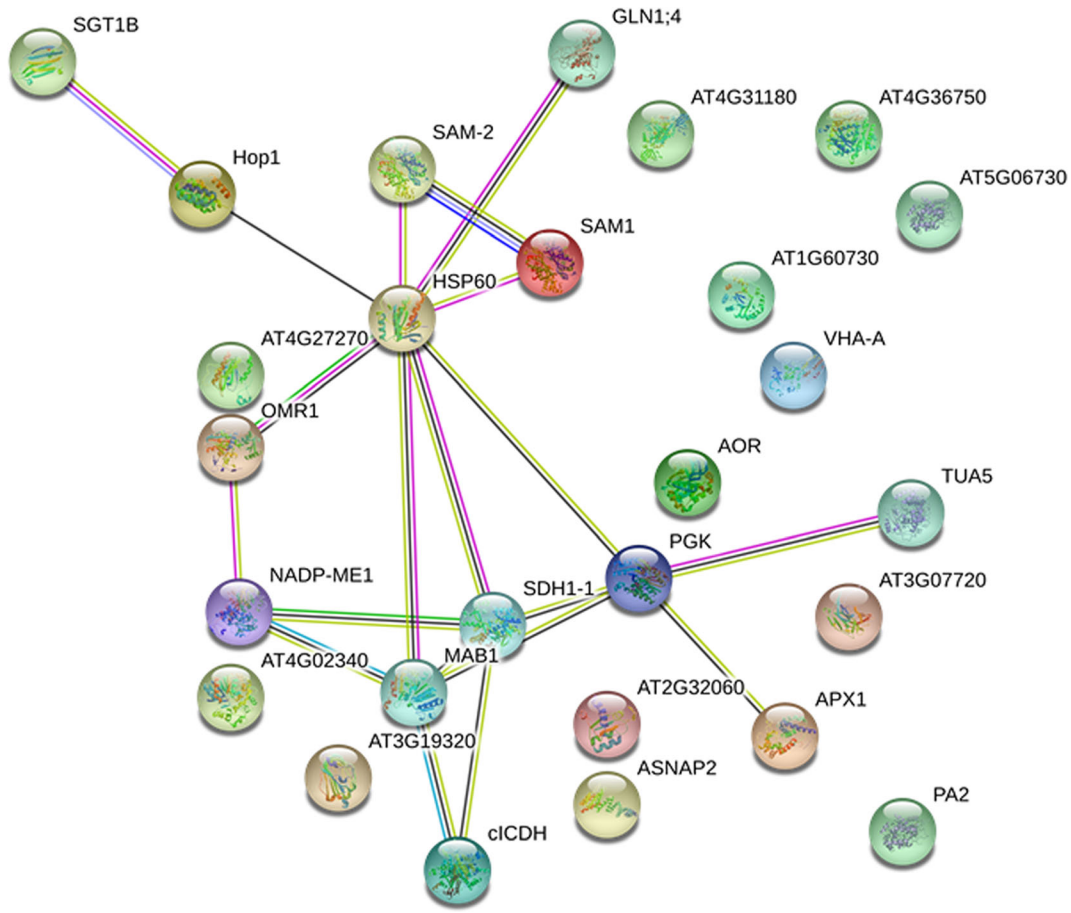

Fig. 4 Interaction network of differentially represented proteins of watermelon root inoculated with *F. oxysporum*. Small nodes mean proteins of unknown 3D structure. Large nodes mean proteins of known or predicted 3D structure. Different line colors indicate the types of protein-protein associations: light blue (from database) and purple (experimentally determined) indicate known interactions; green (gene neighborhood), red (gene fusions), blue (gene co-occurrence), light green (text mining), black (co-expression) and light purple (protein homology) indicate predicted interactions

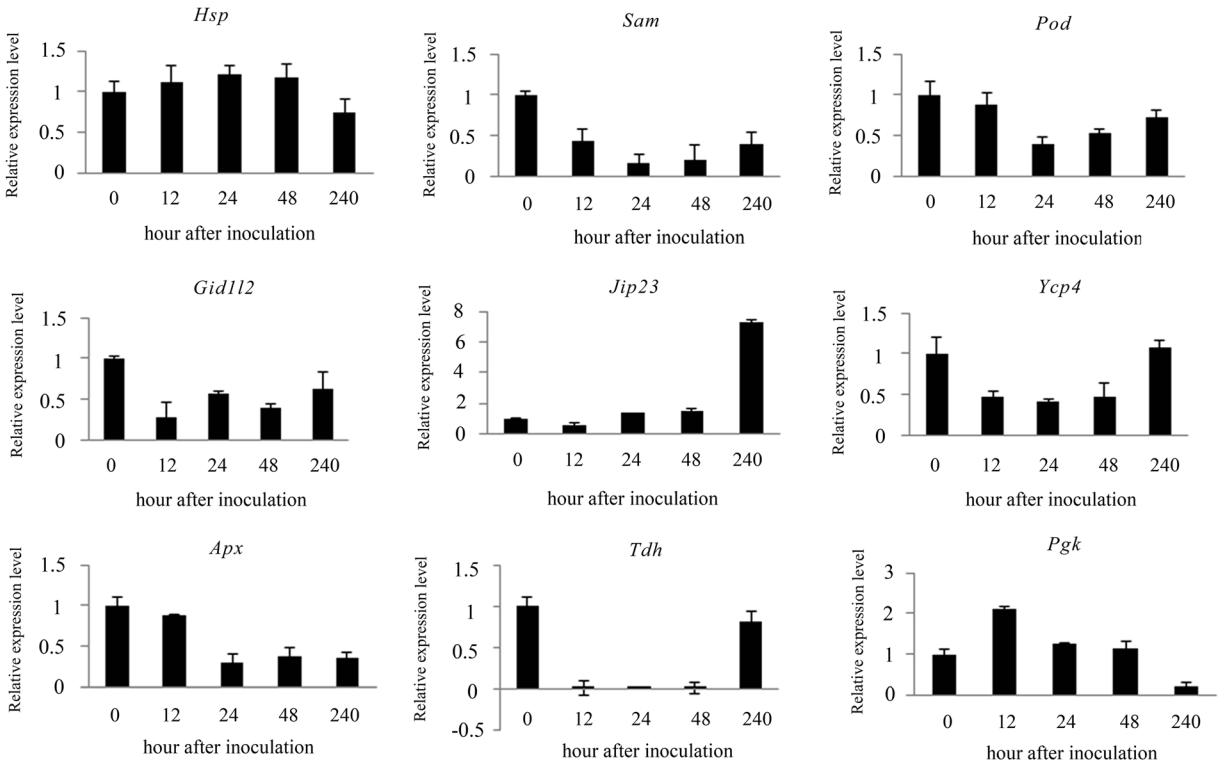

Fig. 5 RT-PCR analysis of the encoding mRNA corresponding to nine selected proteins that with differential changes in abundance in watermelon roots after *F. oxysporum* infection. *Hsp*: heat shock protein; *Sam*: S-adenosylmethionine synthase; *Pod*: peroxidase; *Gid1l2*: gibberellin receptor GID1L2; *Jip23*: jasmonate-induced protein; *Ycp4*: NAD(P)H dehydrogenase (quinone) FQR1-like 2; *Apx*: ascorbate peroxidase; *Tdh*: threonine dehydratase biosynthetic; *Pgk*: phosphoglycerate kinase

In *F. oxysporum*-infected watermelon, NADP-dependent malic enzyme (NADP-ME, spot s21) had greater relative abundance compared to the mock-treated plants. NADP-ME was shown to function in various metabolic pathways in plants (Casati et al. 1999). The specialized role for NADP-ME is its carbon fixation activity in C_4 photosynthesis. Apart from this, NADP-ME also participates in the synthesis of lignin in monolignol biosynthesis, of flavonoids in flavonoid biosynthesis and of activated oxygen species (Casati et al. 1999) after pathogen attack. Lignin has a role in structural reinforcement of plant cell wall, which is the first barrier preventing pathogen penetration (Li et al. 2010). The antimicrobial activity of flavonoids has been well documented in plants under pathogen attack (Treutter 2006). For instance, the increased production of flavonoids has been suggested correlating with higher disease resistance for non-AM white clover (Carlsen et al. 2008). Increased levels of activated oxygen species (AOS), which are often referred to as reactive oxygen species (ROS), can kill or damage pathogens (Casati et al. 1999), whereas excess AOS can also induce plant programmed cell death (Mittler and Zilinskas 2004). Consistent with this, an isocitrate dehydrogenase (spot s22) was over-represented in inoculated watermelon to remove excess AOS to prevent damage to cellular components (Mhamdi and Noctor 2015). Overall, the over-representation of NADP-ME exhibits a role in watermelon defense by providing building blocks and energy for the biosynthesis of defense compounds.

Stress and defense related proteins

Among proteins exhibiting altered levels, heat shock protein (spot s4) and chaperonin CPN60–2 (spot s5) were identified in watermelon infected with *F. oxysporum*. Abundance of both proteins decreased in the inoculated plants. It was previously documented that heat shock proteins (HSPs) act as molecular chaperones in protein folding process by recognizing misfolded proteins and preventing the formation of potential toxic aggregates during stress (Saidi et al. 2009)

or by degrading unstable proteins (Hinault et al. 2006). Based on this observation, Hsp75 accumulated in tomato leaves in response to pathogen infection (Piterková et al. 2013). Opposite results were obtained both in this work and in pathogen-infected cashew stems (Cipriano et al. 2015), which was explained as the pathogen's attempt to infect the host cell by avoiding the triggering of plant self-defense under stress conditions. HSP90 also functioned as an interactor with both SGT1 and RAR1 (Liu et al. 2004). A series of reports documented the critical role of the SGT1-Hsp90 complex for functional *R* genes. Silencing or knockdown one of the functions of this protein complex causes the suppression of R proteins (Shirasu 2009; Kadota et al. 2010). STG1 protein (spot s6) was under-represented in roots of watermelon seedlings infected with *F. oxysporum*. Under-representation of SGT1 might be related to a reduction in reactive oxygen species (ROS) production (Shibata et al. 2011).

A differential representation of oxidoreduction enzymes was observed in watermelon infected with *F. oxysporum*. Three peroxidases (spot s11, s19, s31) and aldo-keto reductase (spot s13) were identified. One peroxidase (spot s11) was under-represented in the inoculated plants. The suppression of peroxidase might be related to the pathogen's ability to modify (Münzenberger et al. 1997) or avoid (Mohr et al. 1998) the host defence responses. Peroxidases (PR-9), which is one of the most widely reported defense-related oxido-reductive enzymes, role essentially in scavenging the ROS (Imahori 2014) that are generated in plant tissues suffering from environmental stimuli. Given their importance in preventing ROS accumulation and repairing cell damage, the under-representation of peroxidases (spot s19, s31) in watermelon may be the result of cellular protection after pathogen attack.

Changes in redox state in watermelon were evidenced by identification of flavoprotein WrbA (spot s26) and NAD(P)H dehydrogenase (quinone) FQR1-like 2 (spot s15). Flavoprotein WrbA (spot s26) is involved in oxidative stress and was over-represented in *F. oxysporum*-infected watermelon compared to the mock-inoculated plants. Flavoprotein wrbA was characterized as having NADH: quinone oxidoreductase activity (Patridge and Ferry 2006), and its expression was up regulated in response to stressors such as salt (Liu et al. 2012), zinc (Romeo et al. 2014) and H_2O_2 (Bian et al. 2015). The over-representation of this protein suggests its potential role in maintaining cell survival under *F. oxysporum* infection.

NAD(P)H dehydrogenase (quinone) FQR1-like 2 (spot s15) was down-represented in *F. oxysporum* infected watermelon, indicating an attempt by plants to accumulate more ROS to strengthen their defense against fungal attack (Heyno et al. 2013). Similar results were observed in *Arabidopsis* (Heyno et al. 2013). The author found that the $fqr1^{-}$ knock-out line showed higher potential antioxidant activities and was more resistant to necrotrophic attack than the wild phenotype.

In watermelon, two Jasmonate-induced proteins (JIPs, spot s18, s27) were over-represented after *F. oxysporum* inoculation. We presume that the up-representation of JIPs might be related to the plants' attempt to maintain their protein balance without changing the average synthesizing capacity for bulk proteins in pathogen-attacked cells (Mueller-Uri et al. 1988).

Amino acid biosynthesis related proteins

Changes in the methyl cycle were evidenced by under-representation of S-adenosylmethionine synthase (SAMs, spot s7, s8, s9) in *F. oxysporum*-infected watermelon. SAM is the sole donor of methyl groups in numerous methylation reactions that modify histones, nucleic acids, and phospholipids (Roje 2006). Lipid methylation is correlated with energy storage and resistance to fungal attack (Schmid and Patterson 1988). Low SAM is associated with lipid accumulation and tissue injury (Ding et al. 2015). Consistent with this finding, the under-representation of this protein in watermelon might be the cause of the wilting morphology in plants.

Two proteins involved in protein synthesis were under-represented. As a structural and functional constituent of the ribosome, the 40S ribosomal protein S12 (spot s25) plays a role in translation. For instance, the 40S ribosomal protein S12 was previously shown to be responsible for the selection efficiency of tRNA molecules during translation (Ochi and Hori 2007). Threonine dehydratase (spot s30) is the rate-limiting enzyme in the L-isoleucine (Ile) biosynthesis pathway. Threonine dehydratase is feedback-inhibited by Ile, and a high Ile concentration can act as an allosteric inhibitor (Mourad and King 1995). The amino acid overproduction is feedback-insensitive and might be a source for plants with higher resistance. The under-representation of these proteins might be related to the plants' attempt to synthesize of proteins involved in watermelon defense against *F. oxysporum*.

Signal transduction proteins

Two proteins, gibberellin receptor GID1L2 (spot s14) protein and LRR-RLK (spot s24) protein, associated with signal transduction were identified. *F. oxysporum* infection reduced the intensity of both proteins. Gibberellins (GA) are well-known developmental hormones, and recent data have suggested their role in modulating host immunity (De Bruyne et al. 2014). As the primary factor mediating GA perception, the GA receptor protein perceives the GA signal and the GA-GID1 complex interacts with the growth-repressing protein DELLA. A quadruple mutant of DELLA led to high levels of SA-dependent resistance in *Arabidopsis* after inoculation with the hemibiotrophic pathogen *P. syringae* (Navarro et al. 2008). Although emerging data support the function of the multifaceted regulator of GAs in plant immunity similar to the other defense hormones SA, JA and ET, further studies are needed to unveil their precise role in plant-microbe interactions (De Bruyne et al. 2014).

Protein kinases play pivotal roles in signaling transduction after the plant sensing of pathogen effectors (Tena et al. 2011). An increased amount of protein kinase was regularly found in plant defence response (Macho and Zipfel 2014). A protein kinase protein was up-represented in cashew challenged with *L. theobromae* (Cipriano et al. 2015). Knockdown of the LRR-RLK encoding leucine-rich repeat receptor-like protein kinase significantly reduced the expression of pathogen defense genes (Parrott et al. 2016). In recent years, RLKs were found as part components of plant pattern recognition receptor (PRR) complexes, and numerous regulators were required to achieve their initiation and fine-tuning of immune responses (Macho and Zipfel. 2014). Tomato LRR-RLK SOBIR1 was observed interact in planta with LRR-receptor like proteins Cf-4 and Ve1. Silencing of SOBIR1 compromised the Cf-4- and Ve1-mediated hypersensitive response and immunity (Liebrand et al. 2013). The plant-specific ankyrin-repeat (PANK) protein XB25 and the ubiquitin ligase XB3 physically interacts with the rice RLK protein XA21 in vitro, and the downregulation of Xb25 or Xb3 resulted in reduced levels of XA21 and compromised XA21-mediated disease resistance (Wang et al. 2006; Jiang et al. 2013). These findings prompt us to hypothesis that the under-representation of LRR-RLK protein (spot s24) observed in our study might also be the result of the reduced intensity of other regulatory proteins, and consequently, compromised LRR-RLK protein (spot s24) mediated immunity.

Transport and cell structure-related proteins

An increase in the abundance of tubulin (spot s20) was identified in watermelon roots inoculated with *F. oxysporum*. Similar observations were documented in cashew stems in response to *Lasiodiplodia theobromae* infection (Cipriano et al. 2015). Tubulin is a typical cytoskeleton-related proteins and helps maintain cell structures. The *F. oxysporum* pathogen penetrated epidermal cell borders by secreting lytic enzymes or forming penetration pegs (Zvirin et al. 2010), which may possibly result in the rearrangement of the cytoskeleton (Sinha and Chattopadhyay 2011). Therefore, it is proposed that tubulin might play a role in the regulation of cell division and thereby maintain the normal cell structure during the early stage of *F. oxysporum* infection.

An alpha-soluble NSF attachment protein (spot s23) was also identified in this work and showed over-representation in response to *F. oxysporum* infection. NSF is an essential enzyme for vesicle trafficking, which performs an essential function in membrane fusion by binding Soluble NSF Attachment Protein (SNAP)-Receptor (SNARE) complexes (Zhao et al. 2011). Recently, it was observed that vesicle trafficking also plays an important role in stress responses (Leshem et al. 2006; Mazel et al. 2004), which implies its potential role in plant adaptation to stress.

Conclusions

F. oxysporum could penetrate into the xylem vessel of root of watermelon and led to visual wilting symptoms at 10 dpi. We used proteomic-based techniques to explore changes in root proteomes during the watermelon-*F. oxysporum* interaction. The identified proteins were involved in several biological processes, most of which function in energy and metabolism, stress or defense, indicating that watermelon roots could directly alter the abundance of these proteins to establish their defense response. These proteomic data provide potential candidate proteins that have great relevance in the biological pathways that linked to watermelon-*F. oxysporum* pathosystem. Further studies will focus on fully understanding the roles of these proteins during *F. oxysporm* infection via transgenic approaches.

Acknowledgements This work was supported by National Industrial Technology System for Watermelon & Melon. Title: Breeding of Grafting Rootstocks for Watermelon & Melon (CARS-NO.26), and Jiangsu Provincial Support Program for Agriculture, 2015 to 2017. Title: Innovation and integrated application of commercial chain techniques of good product direct selling to e-commerce and store in Watermelon [CX(15)1018].

References

Afroz A, Ali GM, Mir A, Komatsu S (2011) Application of proteomics to investigate stress induced proteins for improvement in crop protection. Plant Cell Rep 30:745–763

Baayen RP, Van Eijk C, Elgersma DM (1989) Histology of roots of resistant and susceptible carnation cultivars from soil infested with *Fusarium oxysporum* f. Sp. *dianthi*. Eur J Plant Pathol 95:3–13

Baena-González E, Sheen J (2008) Convergent energy and stress signaling. Trends Plant Sci 13:474–482

Bian YW, Lv DW, Cheng ZW, Gu AQ, Cao H, Yan YM (2015) Integrative proteome analysis of *Brachypodium distachyon* roots and leaves reveals a synergetic responsive network under H_2O_2 stress. J Proteome 128:388–402

Bradford MM (1976) A rapid and sensitive method for the quantitation of microgram quantities of protein utilizing the principle of protein-dye binding. Anal Biochem 72:248–254

Carlsen SCK, Understrup A, Fomsgaard IS, Mortensen AG, Ravnskov S (2008) Flavonoids in roots of white clover: interaction of arbuscular mycorrhizal fungi and a pathogenic fungus. Plant Soil 302:33–43

Casati P, Drincovich MF, Edwards GE, Andreo CS (1999) Malate metabolism by NADP-malic enzyme in plant defense. Photosynth Res 61:99–105

Chang PFL, Hsu CC, Lin YH, Chen KS, Huang JW, Liou TD (2008) Histopathology comparison and phenylalanine ammonia lyase (PAL) gene expressions in fusarium wilt infected watermelon. Aust J Agric Res 59:1146–1155

Cipriano AKAL, Gondim DMF, Vasconcelos IM, Martins JAM, Moura AA, Moreno FB et al (2015) Proteomic analysis of responsive stem proteins of resistant and susceptible cashew plants after *Lasiodiplodia theobromae* infection. J Proteome 113:90–109

De Bruyne L, Höfte M, De Vleesschauwer D (2014) Connecting growth and defense: the emerging roles of brassinosteroids and gibberellins in plant innate immunity. Mol Plant 7:943–959

Ding W, Smulan LJ, Hou NS, Taubert S, Watts JL, Walker AK (2015) *s*-Adenosylmethionine levels govern innate immunity through distinct m ethylation-dependent pathways. Cell Metab 22:633–645

Fernández-garcía N, Carvajal M, Olmos E (2004) Graft union formation in tomato plants: peroxidase and catalase involvement. Ann Bot 93:53–60

Garrett SD (1970) Pathogenic root-infecting fungi. University Press, Cambridge

Guo SG, Zhang JG, Sun HH, Salse J, Lucas WJ, Zhang HY et al (2013) The draft genome of watermelon (*Citrullus lanatus*) and resequencing of 20 diverse accessions. Nat Genet 45:51–58

Heyno E, Alkan N, Fluhr R (2013) A dual role for plant quinone reductases in host-fungus interaction. Physiol Plantaru 149: 340–353

Hinault MP, Ben-Zvi A, Goloubinoff P (2006) Chaperones and proteases: cellular fold-controlling factors of proteins in neurodegenerative diseases and aging. J Mol Neurosci 30:249–265

Imahori Y (2014) Role of ascorbate peroxidase in postharvest treatments of horticultural crops. P. Ahmad (Ed.), Oxidative damage to plants: antioxidant networks and signaling, Elsevier Inc., San Diego, pp 425-451

Jiang Y, Chen X, Ding X, Wang Y, Chen Q, Song WY (2013) The XA21 binding protein XB25 is required for maintaining XA21-mediated disease resistance. Plant J 73:814–823

Kadota Y, Shirasu K, Guerois R (2010) NLR sensors meet at the SGT1-HSP90 crossroad. Trends Biochem Sci 35:199–207

King SR, Davis AR, Liu WG, Levi A (2008) Grafting for disease resistance. Hortscience 43:1673–1676

Leshem Y, Melamed-Book N, Cagnac O, Ronen G, Nishri Y, Solomon M et al (2006) Suppression of Arabidopsis vesicle-SNARE expression inhibited fusion of H_2O_2-containing vesicles with tonoplast and increased salt tolerance. Proc Natl Acad Sci U S A 103:18008–18013

Li X, Bonawitz ND, Weng JK, Chapple C (2010) The growth reduction associated with repressed lignin biosynthesis in *Arabidopsis thaliana* is independent of flavonoids. Plant Cell 22:1620–1632

Liebrand TW, van den Berg GC, Zhang Z, Smit P, Cordewener JHG, America AHP et al (2013) Receptor-like kinase SOBIR1/EVR interacts with receptor-like proteins in plant immunity against fungal infection. Proc Natl Acad Sci U S A 110:10010–10015

Liu Y, Bruch-Smith T, Schiff M, Feng S, Dinesh-Kumar SP (2004) Molecular chaperone Hsp90 associates with resistance protein N and its signaling proteins SGT1 and Rar1 to modulate an innate immune response in plants. J Biol Chem 279:2101–2108

Liu YM, Du HM, He XX, Huang BR, Wang ZL (2012) Identification of differentially expressed salt-responsive proteins in roots of two perennial grass species contrasting in salinity tolerance. J Plant Physiol 169:117–126

Livak KJ, Schmittgen TD (2001) Analysis of relative gene expression data using real-time quantitative PCR and the $2^{-\Delta\Delta CT}$ method. Methods 25:402–408

López-Gresa MP, Maltese F, Bellés JM, Conejero V, Kim HK, Choi YH et al (2009) Metabolic response of tomato leaves upon different plant-pathogen interactions. Phytochem Anal 21:89–94

Macho AP, Zipfel C (2014) Plant PRRs and the activation of innate immune signaling. Mol Cell 54:263–272

Martyn RD (1996) Fusarium wilt of watermelon. In: Zither TA, Hopkins DL, Thomas CA (eds) Compendium of cucurbit diseases. The American Phytopathology Society, St. Paul, MN, pp 13–14

Mazel A, Leshem Y, Tiwari BS, Levine A (2004) Induction of salt and osmotic stress tolerance by overexpression of an intracellular vesicle trafficking protein AtRab7 (AtRabG3e). Plant Physiol 134:118–128

Meru G, McGregor C (2016) Genotyping by sequencing for SNP discovery and genetic mapping of resistance to race 1 of *Fusarium oxysporum* in watermelon. Sci Hortic 209:31–40

Mhamdi A, Noctor G (2015) Analysis of the roles of the *Arabidopsis* peroxisomal isocitrate dehydrogenase in leaf metabolism and oxidative stress. Environ Exp Bot 114:22–29

Miernyk JA, Thelen JJ (2008) Biochemical approaches for discovering protein-protein interactions. Plant J 53:597–609

Mittler R, Zilinskas BA (2004) Activated oxygen species in multiple stress situations and protective systems. In: Sandermann H (ed) Molecular ecotoxicology of plants, Springer. Berlin Heidelberg, New York, pp 51–73

Mohr U, Lange J, Boller T, Wiemken A, Vögeli-Lange R (1998) Plant defense genes are induced in the pathogenic interaction between bean roots and *Fusarium solani*, but not in the symbiotic interaction with the arbuscular mycorrhizal fungus *Glomus mosseae*. New Phytol 138:589–598

Moreira RC, Lima JS, Silva LGC, Cardoso JE (2013) Resistance to gummosis in wild cashew genotypes in northern Brazil. Crop Prot 52:10–13

Mourad G, King J (1995) L-O-Methylthreonine-resistant mutant of Arabidopsis defective in isoleucine feedback regulation. Plant Physiol 107:43–52

Mueller-Uri F, Parthier B, Nover L (1988) Jasmonate-induced alteration of gene expression in barley leaf segments analyzed by in-vivo and in-vitro protein synthesis. Planta 176: 241–247

Münzenberger B, Otter T, Wüstrich D, Polle A (1997) Peroxidase and laccase activities in mycorrhizal and non-mycorrhizal roots of Norway spruce (*Picea abies L.*) and larch (*Larix decidua*). Can J Bot 75:932–938

Navarro L, Bari R, Achard P, Lisón P, Nemri A, Harberd NP et al (2008) DELLAs control plant immune responses by modulating the balance and salicylic acid signaling. Curr Biol 18:650–655

Ochi A, Hori H (2007) Hydroxyl radical probing of rRNA (Gm18) methyltransferase [TrmH]-AdoMet-artificial rRNA ternary complex. Nucleic Acids Symp Ser 51:373–374

Parrott DL, Huang L, Fischer AM (2016) Downregulation of a barley (*Hordeum vulgare*) leucine-rich repeat, non-arginine-aspartate receptor-like protein kinase reduces expression of numerous genes involved in plant pathogen defense. Plant Physiol Bioc 100:130–140

Patridge EV, Ferry JG (2006) WrbA from *Escherichia coli* and *Archaeoglobus fulgidus* is an NAD (P) H: Quinone oxidoreductase. J Bacteriol 188:3498–3506

Piterková J, Luhová L, Mieslerová B, Lebeda A, Petřivalský M (2013) Nitric oxide and reactive oxygen species regulate the accumulation of heat shock proteins in tomato leaves in response to heat shock and pathogen infection. Plant Sci 207:57–65

Roje S (2006) S-adenosyl-L-methionine: beyond the universal methyl group donor. Phytochemistry 67:1686–1698

Romeo S, Trupiano D, Ariani A, Renzone G, Scippa GS, Scaloni A et al (2014) Proteomic analysis of *Populus* × *euramericana* (clone I-214) roots to identify key factors involved in zinc stress response. J Plant Physiol 171:1054–1063

Saidi Y, Finka A, Muriset M, Bromberg Z, Weiss YG, Maathuis FJM et al (2009) The heat shock response in moss plants is regulated by specific calcium-permeable channels in the plasma membrane. Plant Cell 21:2829–2843

Schmid KM, Patterson GW (1988) Effects of cyclopropenoid fatty acids on fungal growth and lipid composition. Lipids 23: 248–252

Shibata Y, Kawakita K, Takemoto D (2011) *SGT1* and *HSP90* are essential for age-related non-host resistance of *Nicotiana benthamiana* against the oomycete pathogen *Phytophthora infestans*. Physiol Mol Plant 75:120–128

Shirasu K (2009) The HSP90-SGT1 chaperone complex for NLR immune sensors. Annu Rev Plant Biol 60:139–164

Sinha R, Chattopadhyay S (2011) Changes in the leaf proteome profile of *Mentha arvensis* in response to *Alternaria alternate* infection. J Proteome 74:327–336

Stenlid MH, Ahlsson F, Forslund A, von Döbeln U, Gustafsson J (2014) Energy substrate metabolism in pyruvate dehydrogenase complex deficiency. J Pediatr Endocrinol Metab 27: 1059–1064

Tena G, Boudsocq M, Sheen J (2011) Protein kinase signaling networks in plant innate immunity. Curr Opin Plant Biol 14: 519–529

Treutter D (2006) Significance of flavonoids in plant resistance: a review. Environ Chem Lett 4:147

Wang YS, Pi LY, Chen X, Chakrabarty PK, Jiang J, De Leon AL et al (2006) Rice XA21 binding protein 3 is a ubiquitin ligase required for full *Xa21*-mediated disease resistance. Plant Cell 18:3635–3646

Yang YJ, Wang LP, Tian J, Li J, Sun J, He LZ et al (2012) Proteomic study participating the enhancement of growth and salt tolerance of bottle gourd rootstock-grafted watermelon seedlings. Plant Physiol Bioc 58:54–65

Yoshimura K, Masuda A, Kuwano M, Yokota A, Akashi K (2008) Programmed proteome response for drought avoidance/tolerance in the root of a C_3 xerophyte (wild watermelon) under water deficits. Plant Cell Physiol 49:226–241

Zhang M, Xu JH, Liu G, Yao XF, Li PF, Yang XP (2015a) Characterization of the watermelon seedling infection process by *Fusarium oxysporum* f.Sp. *niveum*. Plant Pathol 64: 1076–1084

Zhang M, Yang XP, Xu JH, Liu G, Yao XF, Li PF (2015b) Physiological responses of watermelon grafted onto bottle gourd to *Fusarium oxysporum* f. Sp. *niveum* infection. Acta Hortic 1086:107–111

Zhao C, Smith EC, Whiteheart SW (2011) Requirements for the catylytic cycle of the N-ethylmaleimide-sensitive factor (NSF). Biochim Biophys Acta 1823:159–171

Zhou XG, Everts KL, Bruton BD (2010) Race 3, a new and highly virulent race of *Fusarium oxysporum* f. Sp. *niveum* causing fusarium wilt in watermelon. Plant Dis 94:92–98

Zvirin T, Herman R, Brotman Y, Denisov Y, Belausov E, Freeman S et al (2010) Differential colonization and defence responses of resistant and susceptible melon lines infected by Fusarium oxysporum race 1.2. Plant Pathol 59:576–585